PLOS COMPUTATIONAL BIOLOGY

RESEARCH ARTICLE

State-dependent protein-lipid interactions of a pentameric ligand-gated ion channel in a neuronal membrane

Marc A. Dämgen¤, **Philip C. Biggin***

Structural Bioinformatics and Computational Biochemistry, Department of Biochemistry, University of Oxford, Oxford, United Kingdom

¤ Current address: Department of Computer Science, Stanford University, Stanford, CA 94305, USA
* philip.biggin@bioch.ox.ac.uk

OPEN ACCESS

Citation: Dämgen MA, Biggin PC (2021) State-dependent protein-lipid interactions of a pentameric ligand-gated ion channel in a neuronal membrane. PLoS Comput Biol 17(2): e1007856. https://doi.org/10.1371/journal.pcbi.1007856

Editor: Bert L. de Groot, Max Planck Institute for Biophysical Chemistry, GERMANY

Received: April 1, 2020

Accepted: January 7, 2021

Published: February 11, 2021

Data Availability Statement: All relevant data are within the manuscript and its Supporting Information files.

Funding: MAD received funding by the Oxford Wolfson Marriott Graduate Scholarship in Biochemistry, the Studienstiftung des deutschen Volkes, the Goodger and Schorstein Research Scholarship in the Medical Sciences as well as the Vice-Chancellors' fund of the University of Oxford. This project made use of computation time on JADE (EP/P020275/1) via HECBioSim (http://www.hecbiosim.ac.uk), supported by EPSRC (grant no.

Abstract

Pentameric ligand-gated ion channels (pLGICs) are receptor proteins that are sensitive to their membrane environment, but the mechanism for how lipids modulate function under physiological conditions in a state dependent manner is not known. The glycine receptor is a pLGIC whose structure has been resolved in different functional states. Using a realistic model of a neuronal membrane coupled with coarse-grained molecular dynamics simulations, we demonstrate that some key lipid-protein interactions are dependent on the receptor state, suggesting that lipids may regulate the receptor's conformational dynamics. Comparison with existing structural data confirms known lipid binding sites, but we also predict further protein-lipid interactions including a site at the communication interface between the extracellular and transmembrane domain. Moreover, in the active state, cholesterol can bind to the binding site of the positive allosteric modulator ivermectin. These protein-lipid interaction sites could in future be exploited for the rational design of lipid-like allosteric drugs.

Author summary

Ion channels are proteins that control the flow of ions into the cell. The family of ion channels known as the pentameric ligand gated ion channels (pLGICS) open in response to the binding of a neurotransmitter, moving the channel from a resting state to an open state. The glycine receptor is a pLGIC whose structure has been resolved in different functional states. It is also known that the response of pLGICs can also be modified by different types of lipids found within the membrane itself but exactly how is unclear. Here, we used a realistic model of a neuronal membrane and performed molecular dynamics simulations to show various lipid-protein interactions that are dependent on the channel state. Our work also reveals previously unconsidered protein-lipid interactions at a key junction of the channel known to be critical for the transmission of the opening process. We also demonstrate that cholesterol interacts with the protein at a site already known to bind to another compound that modulates the channel, called ivermectin. The work should be useful for future design of allosteric modulators.

EP/R029407/1). PCB thanks the BBSRC (www.bbsrc.ac.uk) for funding (BB/S001247/1). The funders had no role in study design, data collection and analysis, decision to publish, or preparation of the manuscript.

Competing interests: The authors have declared that no competing interests exist.

Introduction

Members of the pentameric ligand-gated ion channel (pLGIC) family are pervasively found in all neurons and their primary function is to mediate neuronal communication [1,2]. They are located in the postsynaptic membrane, where neurotransmitter binding leads to conformational changes that open a channel pore permitting passive ion passage that leads to cell hyperpolarization or depolarization [3]. Their dysfunction is associated with a wide range of neurological diseases such as epilepsy, Parkinson's, Alzheimer's and schizophrenia, and thus they constitute pivotal drug targets [4–6]. In mammals, the pLGIC superfamily consists of the cation-selective, excitatory nicotinic acetylcholine receptors (nAChRs), 5-hydroxytryptamine type 3 receptors (5-HT_3Rs) and a single zinc-activated channel as well as the anion-selective inhibitory γ-aminobutyric acid type A receptors ($GABA_A$Rs) and glycine receptors (GlyRs). Moreover, the invertebrate glutamate-gated chloride channel (GluCl) from *Caenorhabditis elegans* as well as the prokaryotic ion channels from *Gloeobacter violaceus* (GLIC) and *Erwinia chrysanthemi* (ELIC) are other important pLGICs [7].

All pLGICs consist of five subunits that are arranged in a pseudosymmetric manner around the pore axis (see **Fig 1A**). They share a conserved overall architecture: a ligand-binding extracellular domain (ECD), a transmembrane domain (TMD) containing the ion channel pore and an intracellular domain (ICD), which is completely absent in prokaryotic pLGICs. For protein-lipid interactions with the membrane environment, the TMD is of particular interest. Each of the five subunits consists of four membrane spanning helices (M1-M4). These helices can be subdivided into 3 concentric rings with respect to their position in the membrane according to Barrantes [8] (see **Fig 1B**). The inner ring consists of the M2 helices which line the pore through which ions flow. They are shielded from the membrane by the M1 and M3 helices that form the middle ring. The latter are partly in contact with the membrane, being shielded towards the inside by the M2 helices and towards the outside by the M4 helices. The M4 helices make up the outer ring and expose the largest surface area towards the membrane environment and are only shielded from the lipid environment towards the inside by contacts with the M1 and M3 helices from the middle ring.

PLGICs are modulated by their lipid environment, but exactly where lipids bind, and how they act, is poorly understood [9–11]. Via reconstitution experiments, cholesterol (CHOL) and anionic lipids have been demonstrated to be crucial for nAChR function [12–15]. In pure phosphatidylcholine (PC) or phosphatidylethanolamine (PE) membranes, nAChRs bind agonist, but remain in an unresponsive, non-conductive state (that has been termed the uncoupled state). However, ternary mixtures of PC, cholesterol and the anionic lipid phosphatidic acid (PA), completely restore nAChR functionality. Interestingly, binary mixtures of PC/CHOL and PC/PA alone are not sufficient to stabilize a large pool of agonist-responsive nAChRs. Furthermore, from biophysical studies the M4 transmembrane helix has emerged as playing a role as a lipid sensor [16,17]. Since mutations along this helix alter gating, M4-lipid interactions are likely to influence the gating pathway [18–20]. Detailed mechanistic insight at a molecular level remains elusive, but recent experimental evidence supports the so-called M4-M1/M3 lipid sensor model which hypothesizes that enhancing M4-M1/M3 interactions potentiates pLGIC function [21]. These interactions are facilitated by aromatic residues lining this interface [22], but if they are lacking, then lipids could potentially act in a surrogate manner to modulate the enhancement of M4-M1/M3 interactions. Experimental evidence for this hypothesis is provided by studies of GLIC and ELIC in pure PC membranes [21]. ELIC, reconstituted in pure PC membranes, has very few aromatic residues at the M4-M1/M3 interface, just like the nAChR, and is equally unresponsive upon agonist binding. GLIC, on the other hand, has more aromatic residues at the M4-M1/M3 interface and remains functional in pure

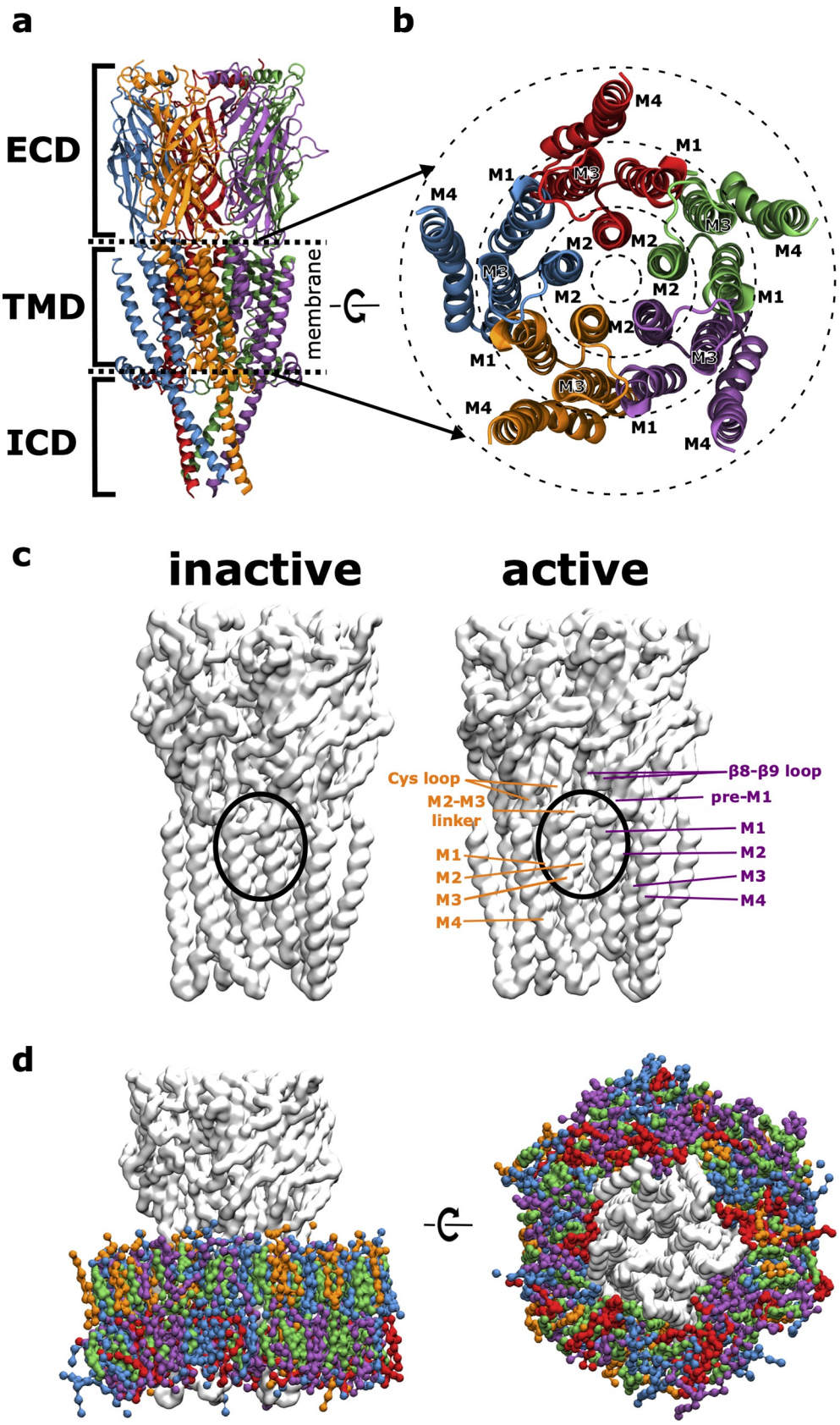
a
b
ECD
TMD
ICD
membrane
M4
M1
M3
M2
c
inactive
active
Cys loop
M2-M3 linker
β8-β9 loop
pre-M1
M1
M2
M3
M4
d

Fig 1. Receptor Architecture and Simulation System. A The overall architecture of pentameric ligand-gated ion channels (pLGICs) with the neurotransmitter binding extracellular domain (ECD), the transmembrane domain (TMD) and an intracellular domain (ICD) (each of the 5 subunits is coloured differently). **B** Detailed view of the transmembrane region from the extracellular side, illustrating how it can be subdivided into 3 regions (dashed concentric rings) according to membrane exposure. **C** Structural comparison of the inactive vs. the active state conformation of the glycine receptor (GlyR), highlighting that in the active state a cleft between the subunit interface opens up, giving the lipid environment access to this site that can also be occupied by the positive allosteric modulator ivermectin. **D** Simulation system viewed in parallel to the membrane plane and from the intracellular side. GlyR (light grey) is embedded in a neuronal model membrane (PC: blue, PE: purple, SM: orange, CHOL: green, PS: red), water and ions are not shown for clarity.

https://doi.org/10.1371/journal.pcbi.1007856.g001

PC membranes. However, by engineering additional aromatic residues at the M4-M1/M3 interface of ELIC, its functionality can be restored. Much of this work has thus far been performed on nAChR, GLIC and ELIC and for the GlyRs it is currently a working hypothesis based on similarity.

Increasingly more structural data of pLGICs with resolved lipids, neurosteroids and detergents is becoming available, providing insights into the molecular details of protein interactions with lipids or lipid-like molecules. Known binding sites for phospholipids are located at the extracellular half of the TMD on the surface of the M1 and M4 helices as seen in a recent $GABA_AR$ structure (PDB 6I53 [23]) or inserted between the M4 helix and the adjacent M1 and M3 helices in several GLIC structures (e.g. PDB 3EAM [24], 6HZW [25]. Phospholipids can also bind at the interface of adjacent subunits at the extracellular TMD half between (+)M3 and (-)M1 as showcased by the crystal structure of GluCl (PDB 4TNW [26] and which overlaps with the binding site of the positive allosteric modulator ivermectin in GlyR (PDB 5VDH [27] and 3JAF [28]) and GluCl (PDB 3RIF [29]). Interestingly, the anionic lipid phosphatidylserine (PS) is a competitor for the ivermectin binding site in GluCl [26], illustrating the competitive nature for lipid occupation on the receptor surface. Moreover, the ivermectin binding site overlaps with the interaction site of neurosteroids. Cholesteryl hemisuccinate is a detergent that is often used to replace cholesterol in crystallization studies and is bound to the ivermectin binding site in a $GABA_AR$ chimera (PDB 5OSA [30]), suggesting that cholesterol itself might be able to interact at the ivermectin binding site. Furthermore, the endogenous neurosteroid allotetrahydrodeoxycorticosterone (THDOC) acts as a potent positive allosteric modulator of $GABA_ARs$ and binds in a similar location. Anionic lipids are found in the intracellular membrane leaflet and accordingly, a phosphatidylinositol 4,5-biphosphate (PIP2) binding site was identified in the intracellular half of the TMD next to the M3 and M4 helices of the α1 subunits in the $GABA_AR$ structure (PDB 6I53 [23]). Two cholesterol molecules have recently been resolved at the intracellular half of theTMD near the M3 and M4 helices of a cryo-EM structure of the nAChR (PDB 6CNJ and 6CNK [31] as suggested previously [21]. An extensive list of all current pLGIC structures with lipids resolved can be found in [10].

While insights from the increasing amount of structural data are valuable, most are obtained under non-physiological conditions. It is not clear for example whether the artificial crystal lattice organization in crystal structures accurately reflects positional preferences of lipids in a natural membrane environment. When *in vivo*, different lipid types compete over interaction sites on the protein surface, but experimental conditions rarely account for this. For example, when obtaining the crystals for GluCl (PDB 4TNW) only 1-palmitoyl-2-oleoyl-sn-glycero-3-phosphocholine (POPC) was added as a single lipid and bound to the ivermectin binding site [26], yet other lipid types might have a higher affinity to this site. Unnatural detergent molecules might preferentially bind to what would be actual lipid sites in a natural membrane environment. The most recent cryo-EM structures of receptors reconstituted in lipid nanodiscs provide the closest mimic to a natural membrane environment, yet the influence of

artificial surface tension on protein structure and dynamics is yet to be determined. It is rare for lipid densities from experimental techniques to allow for unambiguous determination of headgroups or chain length and thus, assignment of the actual lipid type. It is not uncommon that lipid density is simply modelled as a PC molecule with no justification (see for example the supplementary information of [24] or the methods section of [23]). Moreover, lipid interactions are of a highly dynamic nature [32], which poses a limit on the resolution that can be obtained for lipid densities.

Molecular dynamics (MD) simulations provide a complementary tool to experimental techniques that can probe protein-lipid interactions in a natural membrane environment under physiological temperature and pressure [33]. In particular, coarse-grained (CG) MD simulations (using, e.g. the popular Martini model [34]) allow for longer time scales to be explored, which is required to rigorously sample the protein-lipid interaction space [32]. They have been successfully applied to provide structural insights into protein-lipid interactions of key functional membrane proteins, such as transporters [35], ion channels [36] and G-protein coupled receptors (GPCRs) [37] to name a few.

While it is experimentally known that pLGICs are sensitive to their lipid environment and that cholesterol and anionic lipids are both essential for nAChR function, it is still the standard approach to perform simulations of this receptor class in simple bilayer models that only consist of a single lipid class, usually POPC [38,39]. Few simulations have included the functionally crucial lipid types, commonly in very simplified membrane models of binary or tertiary composition with no asymmetry between leaflets [40–42]. Yet, *in vivo*, plasma membranes consist of many different lipid types that are distributed asymmetrically across the leaflets. However, so far no simulations of pLGICs in such a realistic membrane environment have been performed. Based on extensive lipidomics data, Ingollfson et al. [43] have derived a coarse-grained model of a neuronal membrane with asymmetric leaflet composition which can be used as an in vivo-mimetic model for the natural environment of pLGICs.

Here, we have used molecular simulation to reconstitute the GlyR, in an *in vivo*-mimetic neuronal membrane (see **Fig 1D**) and performed CG-MD simulations to probe the protein-lipid interactions. Our membrane model is a simplified version of [43] that consists of representatives for the 5 main lipid types found in neuronal plasma membranes: PC, PE, sphingomyelin (SM), PS, and CHOL. The reduction of the model to these 5 lipid types is necessary to ensure sufficient sampling of the protein-lipid interactions for each lipid type. Yet, it still contains all essential lipid types, particularly the functionally relevant cholesterol and anionic PS, in a typical asymmetric composition of a neuronal membrane. Moreover, to examine possible state-dependent protein-lipid interactions, we have performed two separate sets of simulations, each containing a different state of a human homology model of the α1 GlyR. One is derived from the human inactive (closed) state of α3 GlyR (PDB 5CFB [44]) and one is derived from the active (open) state from the Zebra fish (PDB 3JAE [28]). We chose to use an homology model of human α1 GlyR rather than the GlyR zebrafish cryoEM structures directly, because it is a relevant receptor subtype in humans and is experimentally well characterized [45,46]. The only available pdb coordinates of a GlyR open state (at the time) were the α1 GlyR of zebrafish structure (3JAE). The only closed states available (also at the time) were the α1 GlyR of zebrafish (3JAD) with 3.9 Å resolution and α3 GlyR from human (5CFB) with 3.0 Å resolution. Hence we chose 3JAE as the only available template for the open state and 5CFB with the best resolution for a closed state. The main structural difference in the membrane facing region between the two states is that in the active state, a cleft at the subunit interface is exposed to the lipid environment, which coincides with the binding site of the positive allosteric modulator ivermectin (see **Fig 1C**). Lipid densities reveal that the different conformational states recruit a different lipid environment, thus supporting the view that lipids play a

modulatory role in stabilizing different receptor states. We report previously unreported phospholipid interactions at the ECD-TMD interface that are likely to play a role in stabilizing the tertiary structure in this critical region for signal transduction. Furthermore, cholesterol can bind to the binding site of the positive allosteric modulator ivermectin and thus may itself act as a membrane-intrinsic modulation molecule. Noteworthy is also that the anionic lipid phosphatidylserine (PS) can bind near the intracellular ends of the M3 and M4 helices which overlaps with the PIP2 binding site in human $GABA_AR$, but the details of the headgroup interactions differ. By elucidating a detailed map of the state-dependent protein-lipid interactions with a pLGIC, we provide insights that could be exploited for rational drug development of lipid-like receptor modulators.

Results

To enable sufficient sampling of the lipid distribution around the receptor, we have employed the Martini model [61], which allows for longer simulation times at the cost of less chemical detail (4 heavy-atoms are represented by one "super atom"). In order to be able to characterize the lipid environment that is preferred by the inactive vs. the active state in a computationally feasible way, our approach has been to restrain the receptor in its conformational state, while the lipids were completely free to move and will thus on average yield a distribution that favours this specific conformational state. This strategy has been previously used to characterize state-dependent protein-lipid interactions for a G protein-coupled receptor [37]. The physical logic behind this approach is the same that is commonly used when saying that an agonist stabilizes the active state. In the absence of agonist, there is heterogeneity in the conformational ensemble of the receptor and the receptor will also populate the active state, but less than with an agonist present. Based on the model of conformational selection, the agonist stabilizes the active state by shifting the relative populations towards the active state. In the active state, the affinity for the agonist is higher than in the inactive state. If one would therefore restrain the receptor in the active state, one would observe a higher agonist density in the binding pocket than if one would restrain the inactive state. The same is true for the lipid environment - a certain lipid environment favours the population of the active state over the inactive state and by restraining the receptor to the active conformation, the lipid environment observed on average is the one that most preferably interacts with it and thus stabilizes it.

Cholesterol interactions show dependence on the receptor state

In order to explore in a systematic way where exactly the different lipid types interact with the receptor and whether there a state-dependent differences, we analysed the density of each lipid type around the receptor for both the inactive and active state. First we inspected the 2-dimensional distribution of each lipid type within the membrane for each leaflet (**Fig 2**). A strong colour-gradient between the immediate protein's surroundings and the membrane bulk indicates that the receptor recruits a specific lipid environment at the protein-membrane interface and hot spots that are strongly preferred by certain lipid types can be clearly identified. The key insight from this analysis is that in the active state, CHOL in the extracellular leaflet penetrates deeply between the subunit interfaces (highlighted by circles in **Fig 2**). This is particularly noteworthy, because this is where ivermectin binds to exert its positive allosteric modulatory effect. Another functionally important lipid class for nicotinic acetylcholine receptors are anionic lipids. In our simulations, we have used PS, which which is found only in the intracellular leaflet of neuronal membranes. Hence, a second key observation is that the anionic lipid type PS, is particularly enriched around the receptor surface, indicating very strong protein-lipid interactions. We note, however, that PS is in frequent exchange between

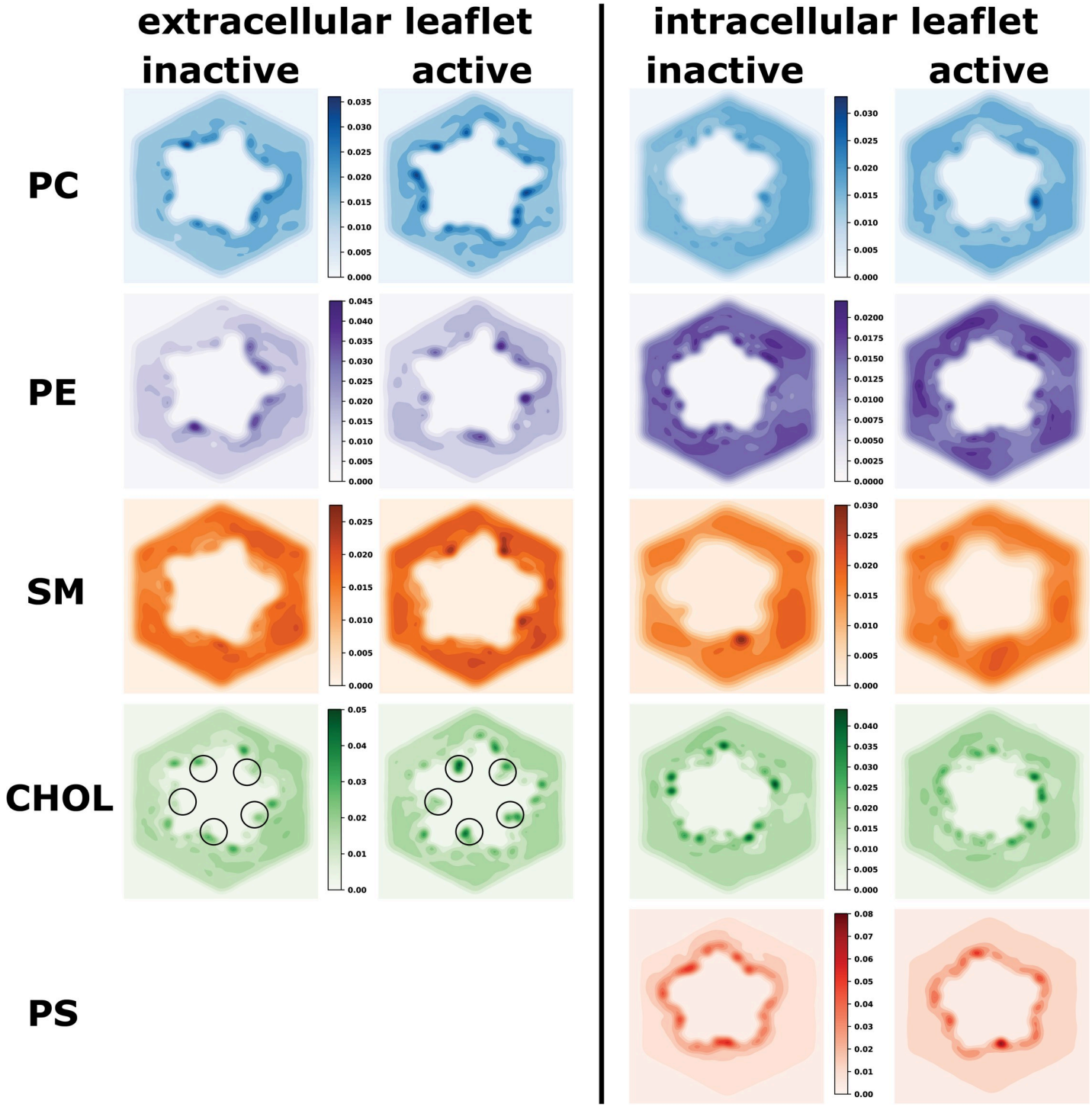

Fig 2. Probability densities of different lipid types around the receptor in the extracellular and intracellular leaflet for the inactive and active state. The colour scales were chosen to highlight the state-dependent differences per leaflet and lipid type. Darker colours represent interaction hotspots. Most striking is that cholesterol in the extracellular leaflet can deeply penetrate the subunit interfaces of the receptor in the active state, which is where the positive allosteric modulator ivermectin binds (indicated by black circles). Moreover, PS is particularly strongly recruited from the membrane bulk towards the receptor surface, indicating very strong protein-lipid interactions. Note that PS is only present in the intracellular leaflet and therefore no density is shown for the extracellular leaflet.

https://doi.org/10.1371/journal.pcbi.1007856.g002

the annular layer and the membrane bulk as showcased by tracking the position of individual PS molecules over time (see S1 Fig). Yet, on average PS strongly prefers direct contact with the receptor.

If simulations were perfectly converged, we would expect to observe C5-symmetry around the 5-fold symmetric receptor. While this is achieved quite well for CHOL (see S2 Fig), this is not quite the case for the other lipid types, which are much less represented in the overall membrane composition and thus likely require longer simulation times to fully converge. This is despite using 10 x 20 μs of simulation time per receptor state and that well exceeds typically reported timescales of CG-MD simulations to study protein-lipid interactions, which are typically in the range of 5–10 repeats of 2–10 μs [37,42].

In order to get a more detailed picture of the protein-lipid interactions of the first lipid shell, we calculated the lipid densities in 3-dimensional space (**Fig 3**). In accordance with **Fig 2**, striking state-dependent changes can be observed for cholesterol. Transitioning from the inactive to the active state allows cholesterol to penetrate into the subunit interface between the crevice of the (+)M3 and (-)M1 helices. Since this is where ivermectin, a known positive allosteric modulator, has been shown to bind, it suggests that cholesterol might act as an intrinsic membrane modulator for receptor activation. This is supported by experimental evidence that cholesterol is crucial for the activation of the nicotinic acetylcholine receptor [6,12,13,15]. Overall, the different lipid types compete with each other for the same interaction regions on the receptor surface. Particularly, the neutral phospholipids PC, PE and SM can all interact with the same parts of the receptor. This is not surprising, as they are chemically more

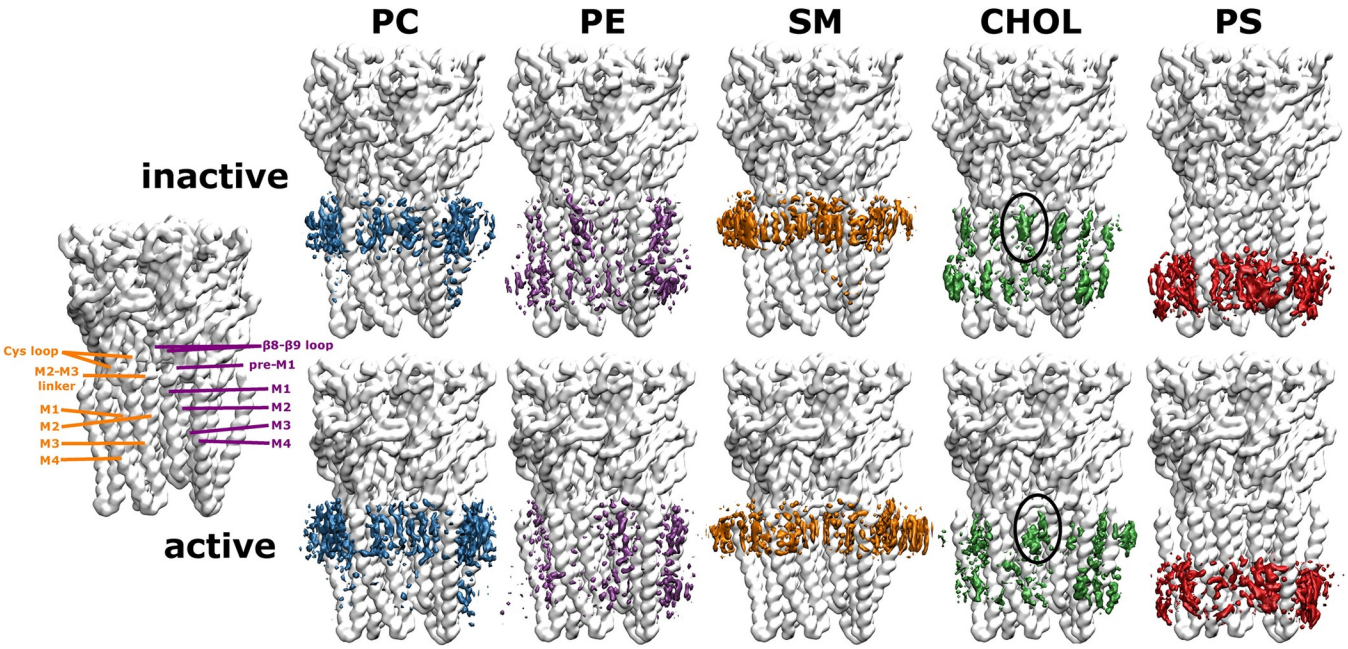

Fig 3. Densities of different lipid types in 3d space for the inactive and active state. For spatial orientation, the receptor structure on the left is labelled with key regions of adjacent subunits - principal (orange) and complementary subunit (purple). In order to better compare the individual lipid type differences for the two conformational states, the densities of each lipid type are shown at different isosurface values, such that they are reweighted as if the membrane consisted of equal amounts of each lipid type (the isosurface for the PC density is shown at a value of 6.3 (6.3) molecules/nm^3, PE density at 5.4 (5.4) molecules/nm^3, SM density at 3.7 (3.8) molecules/nm^3, cholesterol density at 15 (15) molecules/nm^3 and PS density at 5.8 (5.6) molecules/nm^3 for the inactive state (active state)). In the active state, cholesterol can insert itself deep into a crevice that is opening up at the subunit interface between the (+)M3 and (-)M1 helices (position indicated by the black oval), where the binding site for the positive allosteric modulator ivermectin is located, indicating a possible positive modulatory role of cholesterol. The phospholipids PC, PE and SM can all compete for the same regions on the receptor surface, which is not surprising given their similar chemical character.

https://doi.org/10.1371/journal.pcbi.1007856.g003

similar within themselves than compared to the steroid cholesterol or the anionic phospholipid PS.

The duration of protein-lipid contacts reveals a hierarchy between lipid types

As a next step towards a more detailed understanding of the local strength of the protein-lipid interactions, we analysed the binding residues on the receptor for each specific lipid type. Binding residues would typically be identified as those residues with long contact times with lipid molecules. We therefore calculated the average duration of continuous contacts between a molecule of a given lipid species and each protein residue (using a 6 Å cut-off) as a proxy for local binding affinity (and mapped it onto the protein structure in Fig 4**).** Note that this can also be seen as the local residence time for a certain lipid molecule on a specific receptor residue.

The contact duration time analysis reveals a hierarchy between different lipid types: Out of all lipid types, cholesterol engages in the longest contacts with the receptor (see also S3 Fig), indicating its most prevalent role as lipid interaction partner. The second most important lipid type in terms of interaction duration is PS. Finally, PC, PE and SM fall into a similar range of shorter contact times with the receptor. This hierarchy agrees with the experimental insight that cholesterol and a negatively charged lipid type (such as PS) are essential for nAChR function [47]. As expected due to their chemical similarity, PC, PE and SM have very similar contact duration maps. Of note is that only in the active state can CHOL form direct interactions

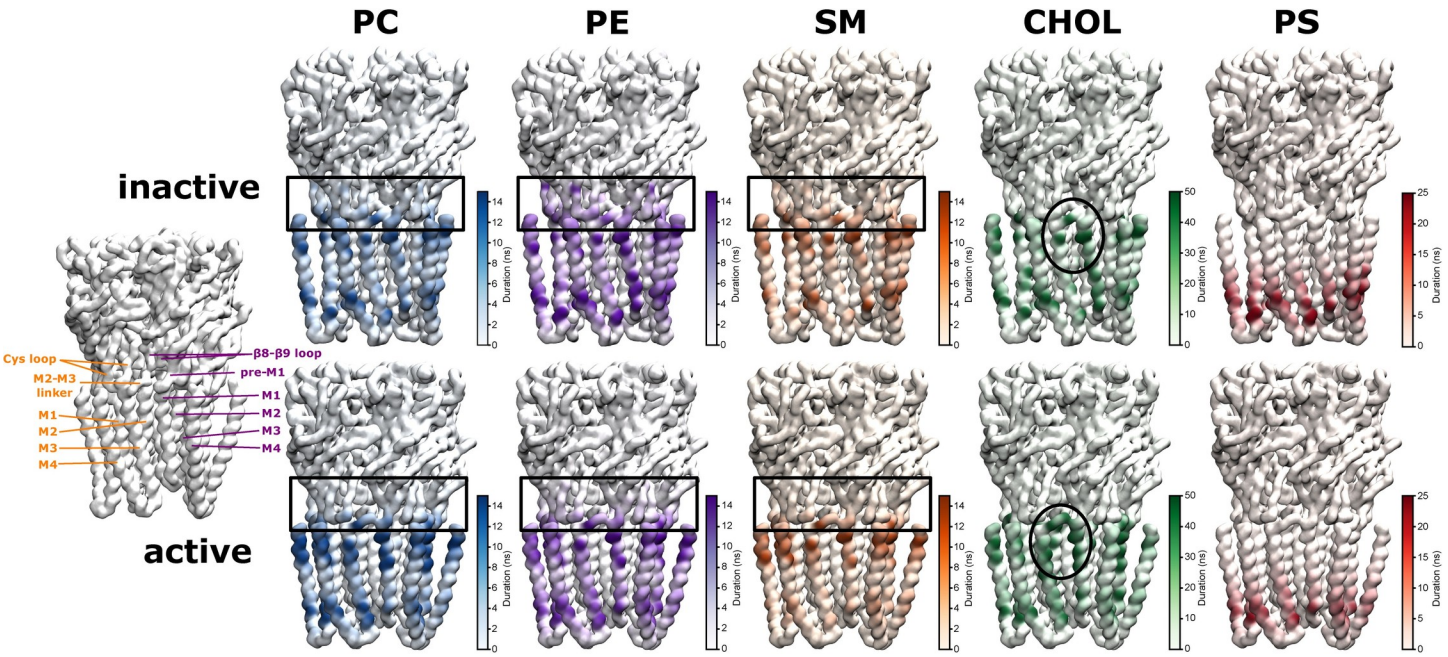

Fig 4. Mean duration of protein-lipid contact per residue for inactive and active state. Key regions of a principal (orange) and complementary subunit (purple) are shown on the left for spatial orientation. The colour scales were chosen so as to highlight the state-dependent differences per lipid type in an optimal way (the maximal contact duration can be longer than the maximum value on the colour scale, see S3 Fig). The per residue-interaction times are a proxy for the local binding affinity of a certain lipid type. Cholesterol forms the longest-lasting contacts with the receptor, followed by the anionic lipid PS, and then the chemically similar phospholipids PC, PE, SM, which supports the experimental evidence that cholesterol and anionic lipids are important for nAChR receptor function. Only in the active state, CHOL can form direct contacts with the pore-lining M2 helix (highlighted by black oval). Interestingly, all phospholipids interact with the ECD-TMD interface (highlighted by black rectangles) which is crucial for signal-transduction from the neurotransmitter binding ECD towards the TMD which contains the channel pore, thus, phospholipids could possibly modulate the conformational changes important for signal transduction at this pivotal interface.

https://doi.org/10.1371/journal.pcbi.1007856.g004

with the pore-lining M2 helix (which are also formed by the positive allosteric modulator ivermectin). Thus, CHOL could directly influence the dynamics of the pore-lining M2 helices. Interestingly, all phospholipids engage in interactions with the ECD-TMD interface, which will be analysed in more detail in the following section.

Membrane lipids can interact with the extracellular domain of the receptor

The ECD-TMD junction of pLGICs is of particular importance for signal transduction, as it is the communication interface between the neurotransmitter binding ECD and the TMD containing the channel pore (see left panel of Fig 5). Neurotransmitter binding is thought to trigger conformational changes in the β8-β9 loop (loop F), the β10 strand that precedes the M1 helix (pre-M1), the β1-β2 loop and the Cys loop (β6-β7 loop) in the ECD that form contacts with the M2-M3 linker of the TMD and thus transduce the signal into opening of the channel pore in the TMD. Note that loop C (β9-β10 loop) that covers the neurotransmitter binding site is known to close due to ligand binding and is directly linked to the β8-β9 loop and the pre-M1 region.

Our simulations show that phospholipids (PC, PE and SM) interact with the receptor at precisely this crucial communication interface (Fig 5). In the inactive state, the phospholipids

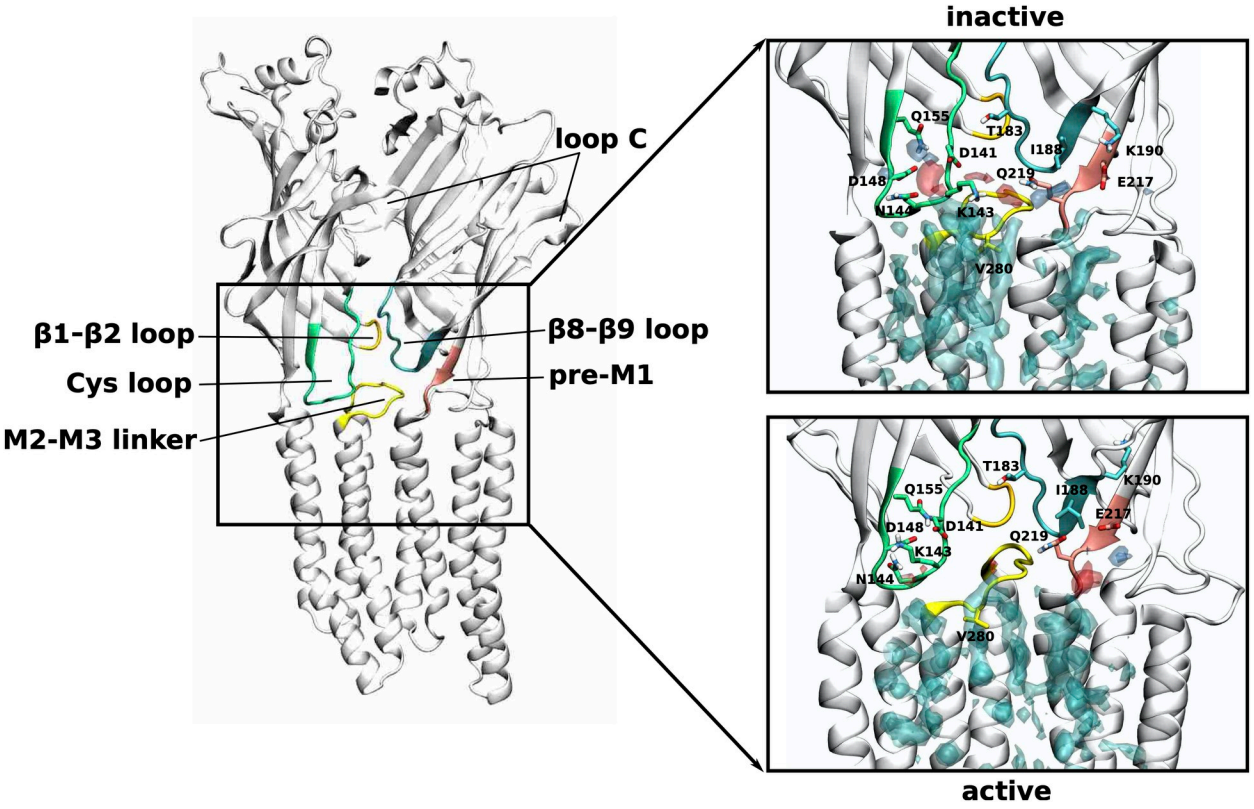

Fig 5. Phospholipid interactions with the ECD-TMD interface. Density arising from the positively charged headgroup beads (choline or ammonium group) is shown in transparent blue, from the negatively charged phosphate headgroup beads in transparent red and from the lipid tails transparent cyan. The densities corresponding to each lipid type are shown at different isosurface values, such that they are reweighted as if the upper membrane leaflet consisted of equal amounts of each lipid type (the isosurface for the PC density is shown at a value of 8.2 (8.2) molecules/nm^3, PE density at 3.8 (3.6) molecules/nm^3, SM density at 6.6 (6.8) molecules/nm^3 for the inactive state (active state)). To show possible atomistic interactions, the initial model used as input to the coarse-grain simulations is shown here just as an indication. In the inactive state, the phospholipid headgroups interact with regions slightly further up towards the extracellular side of the ECD. These interactions are mediated mostly via polar side chains of the Cys loop, the β8-β9 loop as well as the part of the β10 strand that precedes the M1 helix (pre-M1). Note that the latter two are directly connected with loop C whose closing is key to neurotransmitter binding and thus, signal transduction towards the ECD-TMD interface.

https://doi.org/10.1371/journal.pcbi.1007856.g005

preferentially interact with regions further up towards the extracellular side of the ECD. In particular, the Cys loop interacts with the zwitterionic head groups of phospholipids via the charged and polar residues D141, K143, N144, D148 and Q155. Another interaction hot spot is located more towards the complementary subunit, where the headgroups interact with Q219 and E217 from the pre-M1 region as well as T183 and K190 from the β8-β9 loop. The phospholipid densities are overall less far up towards the extracellular side of the ECD in the active compared to the inactive state. Moreover, the phospholipid head group densities are less defined near the Cys loop, indicating more flexibility as well as a weaker interaction strength. In the active state, the phospholipid head group density is much more defined near Q219 and E217 of the pre-M1 region of the complementary subunit, indicating more stable interactions at this site. Furthermore, a more defined lipid binding site appears in the active state at the subunit interface that is not as clearly separated in the inactive state. This density originates mostly from SM (compare also additional density spots of SM at the subunit interfaces in the extracellular leaflet in the active state in Fig 2) and could be due to favourable interactions between SM and CHOL. In summary, the phospholipid density analysis at the ECD-TMD interface suggests that in the inactive state, the phospholipid head groups form more stable interactions with the Cys loop but in the active state they form more stable interactions with the pre-M1 region.

Although for the GlyR, no phospholipid density has been fully resolved in the structures available at present, structural data of other members of pLGIC superfamily with phospholipid or detergent sites at the ECD-TMD interface do exist and a comparison is made in the SI (**S1 Text and S4 Fig**).

Cholesterol can bind to the binding site of the positive allosteric modulator ivermectin

Since CHOL density has been observed at a site that corresponds closely to the binding site of the positive allosteric modulator ivermectin, we analyzed this interaction in more detail. The ivermectin binding site is located between the principal and complementary subunit between the (+)M3 and (-)M1 helices and where ivermectin forms important contacts with the pore lining (+)M2 helix and the (+) M2-M3 linker (**Fig 6 and S1 and S2 Movies**). This site is not accessible in the inactive receptor state, but opens up in the active or desensitized states of the receptor. While cholesterol preferentially interacts at the mouth of the ivermectin binding site in the inactive state, it only deeply penetrates it in the active state, as can be seen in **Figs 2–4.** In the active state, cholesterol density overlaps with the position of structurally resolved ivermectin (**Fig 6A**). Additional fully atomistic simulations reveal that the density we observe in our CG simulations can be assigned to 3 cholesterol molecules (**Fig 6B**), forming stable interactions at this site. Residues previously identified to be involved with ivermectin binding, such as A288 from the (+)M3 helix, I225, I229, P230 and L233 from the (-)M1 helix as well as V280 from the (+)M2-M3 also interact with the density arising from the hydrophobic cholesterol steroid skeleton (**Fig 6**). The additional atomistic simulations reveal that two CHOL molecules can insert between the subunits and overlay with the spiroketal part of ivermectin, while a third CHOL molecule forms interactions with the (+) M2-M3 linker and overlays well with the disaccharide part of ivermectin. The two hydroxy groups of the two inserted CHOL molecules form H-bonds with each other, while the third CHOL molecule can form a H-bond via its hydroxy group with polar backbone atoms of the (+)M2-M3 linker, mostly with the carbonyl group of S278 (**Fig 6**). Interestingly, the polar atoms of ivermectin's disaccharide tail are also orientated towards this region of the (+)M2-M3 linker. The depth of penetration at this site by modulatory molecules is interesting and may be related to their potency as it is also

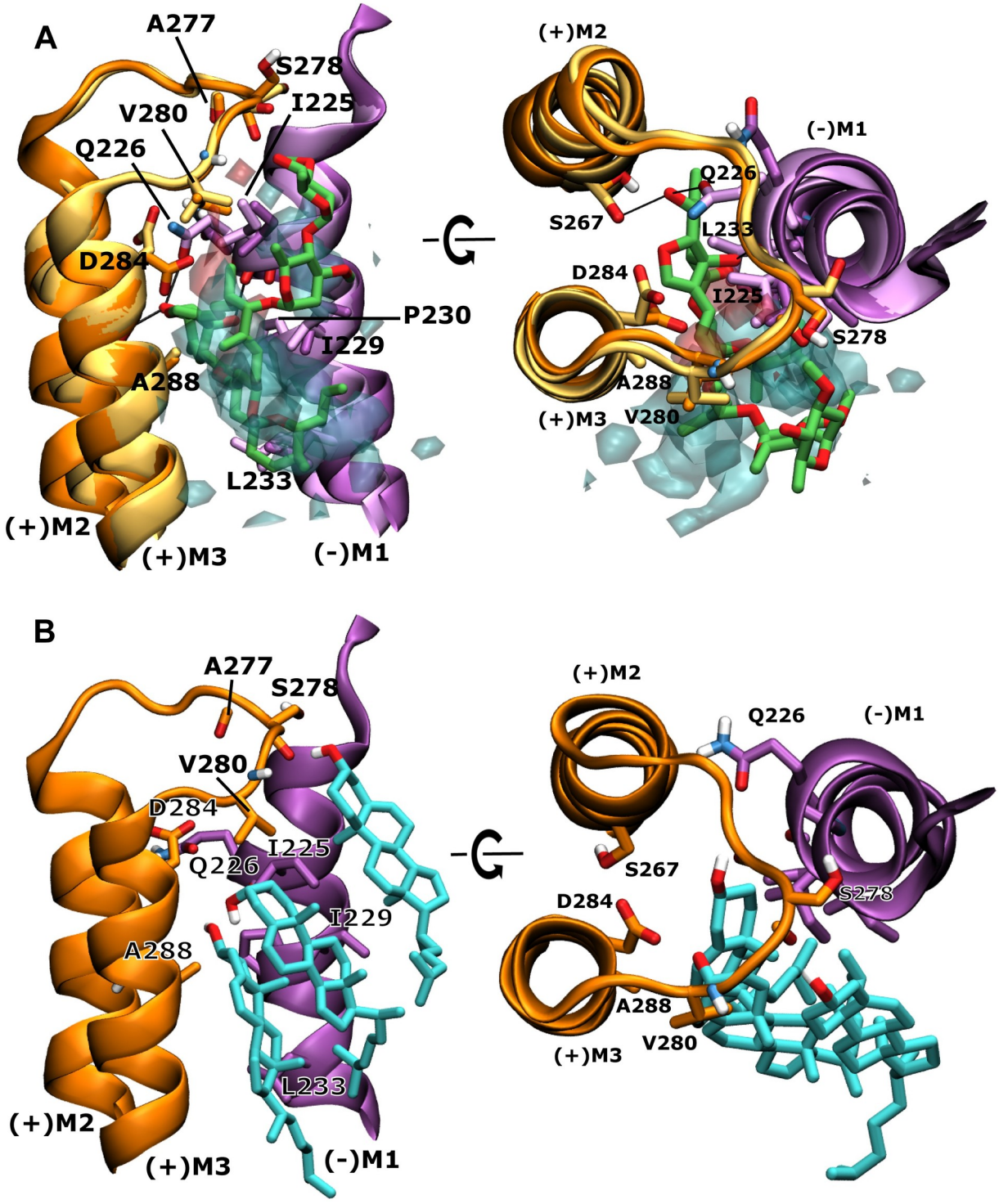

Fig 6. Overlay of cholesterol density with positive allosteric modulator ivermectin at the subunit interface and corresponding binding poses from atomistic simulations. A Overlay of the human α1 GlyR model (darker colours) and cholesterol density (transparent, hydroxy group density in red, remaining hydrophobic steroid skeleton in cyan) from simulations in the active state with the currently highest resolution crystal structure of human α3 GlyR (PDB 5VDH) (lighter colours) with ivermectin (green) bound. Shown is the ivermectin binding site at the interface of adjacent subunits with the (+)M2 and (+)M3 helices of the principal subunit (orange) and the (-)M1 helix of the complementary subunit (purple) forming a crevice and the (+)M2-M3 linker acting as a lid towards the extracellular side. Ivermectin and important residues for ivermectin or cholesterol binding are shown explicitly and key interactions are highlighted by black lines. **B** Representative snapshot of cholesterol binding poses from fully atomistic MD simulations that overlay well with the density observed in CG MD simulations, illustrating that an ensemble of 3 cholesterol molecules can simultaneously interact at this site.

https://doi.org/10.1371/journal.pcbi.1007856.g006

known that ivermectin has higher potency at GluCl, where it is buried *ca*. 1 Å deeper in the cleft than in the human α3 GlyR. Atomistic MD simulations have previously also identified preferred cholesterol binding to the ivermectin binding site in the $GABA_AR$ [41]. However, on a sub-microsecond time scale, the sampling of the highly dynamic interactions was much more limited.

The binding mode of the anionic lipid PS in GlyR differs from the PIP2 binding mode in the $GABA_A$ receptor

Comparison of the PIP2 binding site at one of the α1 subunits of the human α1β3γ2 $GABA_A$ receptor (PDB 6I53) overlaid with the density originating from the anionic lipid PS from our active state simulations reveals the overall location of the anionic binding site is similar at the intracellular end of the M4 and M3 helices (**Fig 7**). However, the binding modes differ between PIP2 and PS. The most striking difference in the receptor structures is that the M4 helix of the GlyR structure maintains its helical secondary structure for 2 more turns towards the intracellular side than the M4 helix of the $GABA_AR$ structure. As a consequence, this region sterically prohibits access of PS in the GlyR, which is precisely where the inositol-1,4,5-trisphosphate (InsP3) head group of PIP2 interacts extensively with the protein backbone of the $GABA_AR$. Moreover, the positively charged side chains of $GABA_AR$ (R249, K312, R313) that electrostatically stabilize the negatively charged InsP3 head group of PIP2 in this region are either not present in human α1 GlyR or in orientations too far away to engage in such interactions (R249 and R309). In GlyR, the negatively charged phosphatidylserine headgroup of PS forms stable electrostatic interactions slightly further towards the extracellular side of the M4 helix with the positively charged side chains R391 and K394. Furthermore, the InsP3 headgroup of PIP2 is overall larger and carries a three-fold negative charged, whereas the phosphoserine headgroup of PS is smaller and carries only a single charge, which is also likely to have an effect on the different binding locations for these headgroups.

Discussion

We have computationally reconstituted the GlyR in a realistic model of a neuronal membrane and performed CG-MD simulations to probe and characterize the molecular level detail of the protein-lipid interactions in two key functional receptor states (inactive and active). Our simulations reveal details of lipid-type specific receptor interactions and show that some key lipid interactions are dependent on the receptor state. This suggests that the lipid environment itself might play an active role in regulating the activation of the receptor. Of particular note, we characterized so far unreported protein-lipid interactions at the ECD-TMD interface, suggesting that lipids might play a modulatory role at this communication interface in the activation process of the receptor. Furthermore, our simulations show that cholesterol binds to the binding site of the positive allosteric modulator ivermectin, indicating that cholesterol might also have a positive modulatory function. Finally, we identify a binding site for the anionic lipid PS at the intracellular leaflet half of the TMD on the surface of the M4 and M3 helices which roughly coincides with the location of PIP2 binding in human $GABA_AR$. This region was also identified as important for the binding of PE to ELIC [17].

The nAChR is the best studied member of the pLGIC superfamily with regards to protein-lipid interactions [48]. Cholesterol and anionic lipids have both been shown to be essential for nAChR function [12–15]. nAChR reconstituted in pure PC or PE membranes bind agonist, but do not open. The unresponsive state of nAChR has been called the uncoupled state. However, mechanistic insight into the molecular details that characterize the uncoupled vs. the responsive (or coupled) state has been elusive so far. Lipid dependency seems to be an

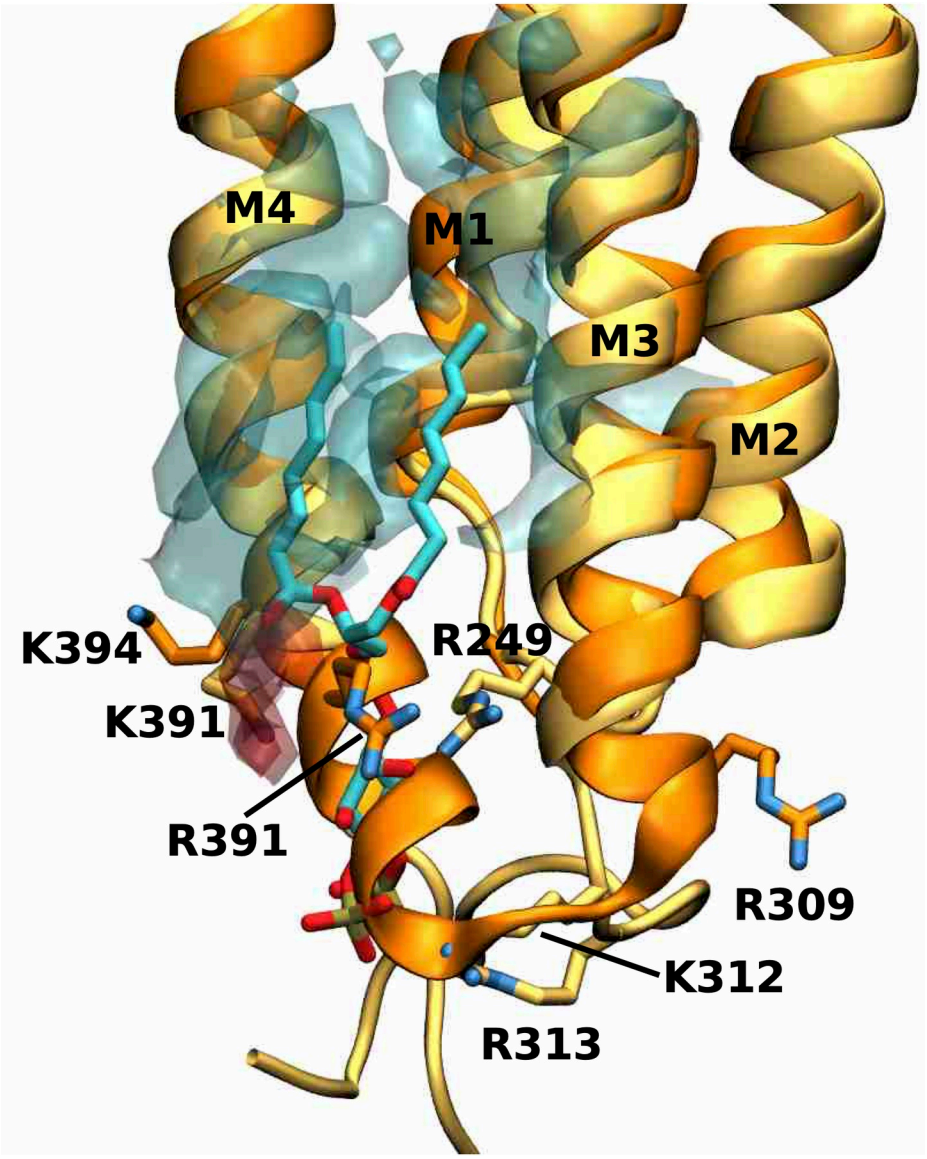

Fig 7. Overlay of PS density with PIP2 near the M4 helix. Overlay of the human α1 GlyR model (darker colours) and PS density (transparent, negatively charged head group density in red, lipid tail density in cyan) from simulations in the active state with the cryo-EM structure of human α1β3γ2 $GABA_A$ receptor (PDB 6I53) (lighter colours) with PIP2 bound. Shown is the PIP2 binding site at one of the α1 subunits. PIP2 and important residues for anionic lipid binding are shown explicitly.

https://doi.org/10.1371/journal.pcbi.1007856.g007

important theme for the whole pLGIC superfamily, as the function of $GABA_A$Rs is also dependent on cholesterol levels [49].

Since current evidence suggests that lipids can modulate nAChR function via interactions with the M4 helix as well as the adjacent M1 and M3 helices, the so called M4 lipid-sensor model has emerged [21]. It hypothesizes that the uncoupled state is structurally characterized by the M4 helix being more distant to its neighbouring M1 and M3 helices and thus the extracellular post-M4 cannot form interactions with the Cys loop of the ECD. Lipids could influence the binding of the M4 helix to the adjacent M1/M3 surface and thus either favour the coupled or uncoupled state [50]. As aromatic residues lining the contact interface of the M4

and M1/M3 helices have been shown to be the main driving force of M4 helix binding to the M1/M3 surface during the folding of GlyR [22], it has further been hypothesized that the varying number of these π-π interactions in pLGIC members is linked to the degree of dependence on the lipid environment [21]. The more aromatic residues support the M4-M1/M3 binding, the less dependent is a receptor on its lipid environment. This hypothesis was given further support recently by elegant work on the ELIC channel which revealed a lipid binding site in this region, which can be linked to the intrinsic flexibility of the M4 helix [17].

Fig 8 gives an overview of the varying degree of aromatic residues lining the M4-M1/M3 interface across representatives of the pLGIC superfamily. In the human α1 GlyR aromatic residues line the M4-M1/M3 interface (**Fig 8A**) in an evenly distributed manner, leading to a tight binding of the M4 helix to the M1/M3 interface and thus, according to the M4 lipid-sensor model, suggesting little dependence on the lipid environment. A similarly aromatic rich interface is found in the β3 $GABA_AR$ (**Fig 8B**). The prokaryotic channel GLIC has only 8 aromatic residues at the M4-M1/M3 interface with a striking gap at the extracellular half of the TMD (**Fig 8C**), indicating weaker binding of the upper half of the M4 helix. On the other end of the spectrum are the nAChR (α4 subunit shown in (**Fig 8D**)) and ELIC (**Fig 8E**) with only 6 and 4 aromatic residues, respectively, suggesting a weak binding of the M4 helix and the M4 lipid-sensor model would predict a strong dependence on the lipid environment. Indeed, nAChR and ELIC have been demonstrated to be highly dependent on their lipid environment and do not undergo agonist-induced opening in minimal PC membranes, whereas GLIC remains functional [21]. While experimental data for GlyR and $GABA_AR$ in this respect are not available, their larger number of aromatic contacts along the M4-M1/M3 interface than GLIC suggest that they would remain functional in minimal PC membranes.

Interestingly, the analysis of aromatic contacts at the M4-M1/M3 interface explains our observation that phospholipids bind to the membrane facing surface of the M1 and M4 helices of GlyR rather than inserting in between the M4-M1/M3 interface. The plethora of aromatic contacts between the M4 helix and the M1/M3 surface binds the M4 helix strongly to the receptor in GlyR. This may also be the reason why similar surface binding of phospholipids is observed in the aromatic-rich $GABA_AR$.

The interpretation of our results requires consideration of the limitations of the coarse-grain simulation approach and the available experimental structures from which we constructed our models. The Martini force field allows for longer simulations that can provide converged lipid distributions, but involves a simplification of chemical detail. For example phospholipids (PC, PE, SM) are extremely similar in Martini: PC and SM both have a phosphocholine headgroup, while PE has a phosphoethanolamine headgroup, which is chemically very similar. Note that in the coarse-grained Martini force field employed here, these groups only differ by single bead (particle type), namely 'Q0' for the choline group in PC and SM, and 'Qd' for the ammonium group in PE. Moreover it has been reported that the Martini model tends to overestimate the strength of protein-lipid interactions. Finally, the only active state structure of GlyR (3JAE) available at the time of manuscript submission has been annotated to a rather "super open state" that might not be physiologically relevant by a recent paper [51].

The protein-lipid interactions described here form the basis for further experimental studies to address their physiological functional consequences *in vivo*. From a pharmacological perspective, the detailed picture of protein-lipid interactions for the GlyR as a pLGIC representative forms the basis to guide future design principles for lipid-like drugs that can partition into the membrane and bind to allosteric sites within the TMD or even at the ECD-TMD interface.

With the ongoing cryo-EM structural revolution, our structural knowledge of interacting lipids with pLGICs will undoubtedly increase with more high resolution structures being

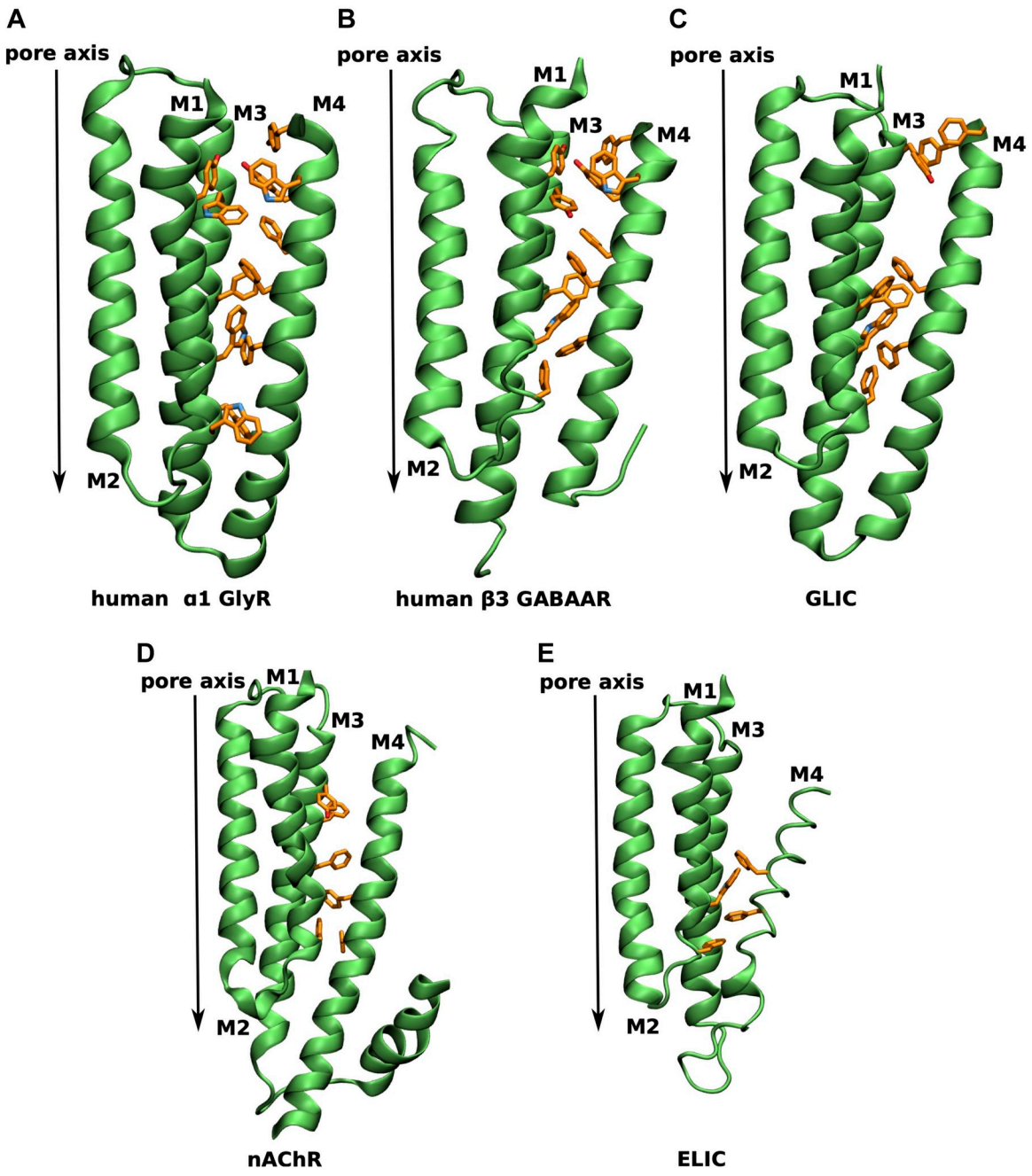

Fig 8. Aromatic residues at the M4-M1/M3 interface of different pLGICs. TMD region of a single subunit viewed in parallel to the membrane plane with aromatic residues at the M4-M1/M3 interface explicitly shown in orange for **A** human α1 GlyR (human homology model from PDB 3JAE [28]), **B** human β3 $GABA_A$ receptor (from PDB 6I53 [23]), **C** GLIC (from PDB 6HZW [25]), **D** α4 human nicotinic acetylcholine receptor (from PDB 5KXI [52]) and **E** ELIC (from PDB 2VL0 [53]).

https://doi.org/10.1371/journal.pcbi.1007856.g008

resolved that show electron density for lipid molecules. Since it is still difficult to identify the exact lipid type from the electron density data alone, MD simulations will be an important complementary technique in order to both identify the molecular identities of the lipid electron density as well as provide insight into the dynamic lipid interactions with the receptor [10].

Methods

Homology modelling

The model of the active conformation of human α1 GlyR was constructed from the structure of *Danio rerio* α1 GlyR (glycine-bound open state; PDB: 3JAE [28]) as previously reported [54]. The model in the inactive conformation was based on the *human* α3 GlyR (strychnine-bound closed state; PDB: 5CFB [44]). Sequences were aligned using Muscle [55] and adjusted manually. 100 models were generated via MODELLER version 9.16 [56] and from the intersection of the top 10 of both molecular PDF and DOPE scores [57], the model with the best QMEAN score [58] was chosen for simulation. The pdb2gmx tool of Gromacs 5.1 [59] was used to add hydrogens with standard protonation states at pH = 7.4. As the sequence identity of the regions excluding the ICD, which is not resolved in the template structures, between human α1 GlyR and zebrafish α1 is 92% and between human α1 GlyR and human α3 is 93%, the model is expected to be of high quality and the protein conformation is not expected to change significantly due to the small number of substitutions. To evaluate the stability of these models, fully atomistic simulations were performed that support their high quality, as evidenced by a low Cα-RMSD around 2–3 Å (see **S5 Fig**), meaning that they remain close to the original structures.

System set up

The homology models of GlyR were converted to coarse-grained MARTINI representations via martinize [61]. Using the insane script [60], each of the coarse-grained protein structures was separately embedded in an asymmetric neuronal model membrane using a hexagonal prism as the periodic simulation box, solvated in water and sodium and chloride ions were added to neutralise the net charge and simulate a physiological concentration of 150 mM (see **Fig 1**). The membrane model is based on [43] and was simplified to consist of representatives of the five most essential lipid species as specified in **Table 1**. For each receptor state, 10 systems were set up with the same number of molecules per species, but with different random seeding of the lipid positions in the membrane plane to improve sampling. No constraints were imposed to maintain the asymmetric lipid distribution across leaflets, but based on previous experience only cholesterol can interchange the leaflets on timescales of tens of μs. The inactive state systems contained 289 lipid molecules and 6621 water and ion molecules, which together with the protein resulted in a total number of 13601 coarse-grained MARTINI beads. The active state systems contained 284 lipid molecules and 6512 water and ion molecules, which together with the protein, resulted in a total number of 13436 coarse-grained MARTINI beads. This resulted in simulation systems with at least 3 lipid shells surrounding the receptor.

Coarse Grained Molecular Dynamics (CG-MD) simulations

All CG-MD simulations were performed with the Martini force field version 2.2 for protein and version 2.0 for lipids [61]. Gromacs 2018 [59] was used as molecular dynamics engine for

Table 1. Composition of a human neuronal model membrane (simplified to 5 essential lipid types based on the model by Ingolfsson *et al* [43]).

Lipid species	Extracellular / mol %	Intracellular / mol %	Total / mol %
POPC	24.4	13.7	19.2
POPE	11.1	21.5	16.2
DOPS	0	16.9	8.3
SM	19.9	3.0	11.6
Cholesterol	44.7	44.9	44.8

https://doi.org/10.1371/journal.pcbi.1007856.t001

all simulations and periodic boundary conditions were applied in all three spatial dimensions. After energy minimisation, the systems were simulated at 310 K and 1 bar for 40 μs. Simulation details were based on the recommended new-rf.mdp parameters [34] and appropriately adjusted. Harmonic restraints with a force constant of 1,000 $kJmol^{-1}nm^{-2}$ were placed on all protein particles to preserve the conformational state close to the original crystal or cryo-EM structure. While this could also be achieved with the ELNEDYN elastic network approach [62] we opted for position restraints for sampling reasons. Using a fixed, single conformation that is most representative for the active or inactive state improves the sampling of protein-lipid interactions. The lipid environment of the receptor then only needs to sample lipid distributions with respect to a single conformation. The closed and open conformational state obtained by structure determination represent the most important (most populated) inactive and active state and are therefore the best representative choice to study the inactive or active state. Allowing for protein flexibility via an elastic network approach would require much longer simulation times to achieve the same degree of convergence, because then the lipids need to sample distributions with respect to many slightly different conformations that constitute a global state (inactive or active). This is based on the assumption that similar lipid localization is expected for both position-restraints and elastic network approaches. To substantiate this assumption, we have run control simulations with an ELNEDYN elastic network and indeed find similar lipid localization for both approaches as exemplified for cholesterol in **S6 Fig**.

Atomistic molecular dynamics simulations

For atomistic simulations, the coarse-grained systems were backmapped to atomistic coordinates with "backward" [63] and the receptor structures replaced by the original homology models. 3 repeats per state were performed with production runs of 1500 ns length each. For the active state simulations, minimally invasive flat bottom restraints between selected atoms were used to keep the channel pore open, as previously reported in detail by us [39]. Atomistic simulations employed the AMBER99SB-ILDN [64] force-field for protein and ions, TIP3P for water [65], and the Slipids parameter set [66–68] for lipids. Glycine ligands used the Horn parameter set [69]. Bulk conditions were mimicked via the use of periodic boundary conditions in all three spatial dimensions. The temperature was maintained at 310 K with the Bussi thermostat [70] using a coupling constant of 0.1ps. A constant pressure of 1 bar was maintained with a Parrinello-Rahmann barostat [71] coupled to the system in a semi-isotropic manner. The time constant used for pressure coupling was 1 ps and the isothermal compressibility set to 4.5×10^{-5} bar^{-1}. The van der Waals interactions were cut off at 10 Å and a dispersion correction was applied to energy and pressure. Electrostatic interactions were treated using the smooth Particle Mesh Ewald (PME) method [72–73], where the real space contribution was cut off at 10 Å and the reciprocal energy term obtained in k-space was calculated on a grid with 1.2 Å spacing using 4th order B-splines for interpolation. The LINCS algorithm [74], was used constrain all bonds with hydrogens, allowing for a time step of 2 fs. Coordinates were written out every 10 ps.

Analysis and visualization

Trajectory analysis and probability density calculations were performed on the last 20 μs out of a total of 40 μs simulation time using frames at a separation of dt = 10 ns and averaged over all 10 repeats per conformational state. The contact-duration data was additionally averaged over all five subunits. A cut-off of 6 Å (corresponding to the first lipid shell) was used to define a protein-lipid contact. Software used for analysis was MDAnalysis [75], MDTraj [76] and in-

house scripts, part of which are now publicly available on https://github.com/wlsong/PyLipID. Visualization was performed in VMD [77].

Supporting information

S1 Text. Comparison of lipid binding sites to other pLGIC members.
(DOCX)

S1 Fig. Trajectories of single DOPS molecules in the membrane plane for the inactive state. Exemplary data shown for 4 DOPS molecules from repeat 1 of the inactive state simulations. Each scatter plot illustrates the movement of a single DOPS molecule over 20 μs of simulation (last 20 μs out of 40 μs total simulation time). Each circle in the scatter plots represents the position of a single DOPS molecule at every 10 ns of simulation time (a transparent shading is used for the circles, so as to highlight preferred lipid locations resulting in darker colours from overlapping circles). Clearly, in a single simulation repeat a single DOPS molecule leaves the receptor surface multiple times and samples large areas of both receptor surface as well as in the membrane (See also Fig 2 of the main manuscript).
(PDF)

S2 Fig. Probability densities of cholesterol for each individual simulation repeat around the receptor in the extracellular and intracellular leaflet for the inactive and active state. The colour scales were chosen to highlight the state-dependent differences per leaflet and lipid type. Darker colours represent interaction hotspots. The initial positions of lipid molecules in each simulation repeat were assigned randomly in order to generate different starting conditions and thus ensure overall a better sampling of lipid mixing. Similar interaction hot spots emerge in the individual simulation repeats, although with different intensity due to the limited sampling time of each individual simulation repeat. Averaging over all 10 simulation repeats, however, yields a rather converged density map of the lipid distribution. (See also Fig 2 of the main manuscript).
(PDF)

S3 Fig. Mean duration of protein-lipid contact per residue for inactive and active state. Averaged over last 20 μs (out of 40μs) of 10 repeats per conformational state and over the 5 subunits. A cut-off of 6 Å is used, which corresponds to the first lipid shell.
(PDF)

S4 Fig. Overlay of phospholipid densities at the ECD-TMD interface with experimental structures. Overlays of the human α1 GlyR model (darker colours) and phospholipid density (transparent, phosphate headgroup density in red, choline/ammonium headgroup density in blue, tail density in cyan) from simulations in the active state with experimentally resolved structures of the pLGIC superfamily (lighter colours) with phospholipid or detergent bound. Three binding sites are observed in simulations (labelled 1, 2 and 3). Lipid binding has been observed in the corresponding regions of sites 1 and 2 for other members of the pLGIC family, but site 3 may be specific to the GlyR. a Overlay with GLIC crystal structure (PDB 6HZW) which has a detergent molecule bound that interacts with its polar headgroup with the Cys loop, while its hydrophobic tail mainly interacts with the M3 helix. b Overlay with GLIC crystal structure (PDB 6HZW) which has a phosphocholine lipid bound that interacts with its polar headgroup with the pre-M1 region as well as the Cys loop, while its hydrophobic tails bridge the interface between the M4 and M1/M3 helices. c Overlay with the α1 subunit of the human $GABA_A$ receptor cryo-EM structure (PDB 6I53), which has a phospholipid bound that interacts with its polar headgroup with the pre-M1 region, while its hydrophobic tails interact

mainly with the M1 helix. d Overlay with the β3 subunit of the human $GABA_A$ receptor cryo-EM structure (PDB 6I53), which has a phospholipid bound that interacts with its polar head-group with the pre-M1 region, while its hydrophobic tails interact with both the M1 and M4 helices.
(PDF)

S5 Fig. Cα-RMSD of inactive and active state homology models in fully atomistic simulations. Darker colours: moving average, lighter colours: original, unsmoothed values. Both states exhibit a similar, low level of flexibility and remain close (around 2–3 Å) to the starting model, supporting the high quality of the homology models.
(PDF)

S6 Fig. Probability densities of cholesterol around the receptor in the extracellular and intracellular leaflet for the inactive and active state obtained with position-restrained approach and elastic network approach. The data for the position-restrained approach (top 4 panels) is also presented in Fig 2 in the main text. The data for the elastic network approach (bottom 4 panels) is based on 5 simulation repeats of 2 μs length for each the active and inactive simulation systems. Similar lipid locations for the position-restrained and elastic network approach can be observed. This substantiates the assumption that both approaches lead to similar lipid distributions.
(PDF)

S1 Movie. Side view of rock and roll movie of cholesterol overlaid on ivermectin binding site.
(MPG)

S2 Movie. Top view of rock and roll movie of cholesterol overlaid on ivermectin binding site.
(MPG)

Acknowledgments

We thank our colleagues Wanling Song, Irfan Alibay and Anna Duncan for useful discussions, and Mark Sansom for additional compute time.

Author Contributions

Conceptualization: Marc A. Dämgen, Philip C. Biggin.

Data curation: Marc A. Dämgen, Philip C. Biggin.

Formal analysis: Marc A. Dämgen, Philip C. Biggin.

Funding acquisition: Marc A. Dämgen, Philip C. Biggin.

Investigation: Marc A. Dämgen.

Methodology: Marc A. Dämgen, Philip C. Biggin.

Project administration: Philip C. Biggin.

Resources: Philip C. Biggin.

Software: Marc A. Dämgen.

Supervision: Philip C. Biggin.

Validation: Marc A. Dämgen.

Visualization: Marc A. Dämgen.

Writing – original draft: Marc A. Dämgen.

Writing – review & editing: Marc A. Dämgen, Philip C. Biggin.

References

1. Cecchini M, Changeux J-P. The nicotinic acetylcholine receptor and its prokaryotic homologues: Structure, conformational transitions & allosteric modulation. Neuropharmacology. 2015; 96, Part B:137–49. https://doi.org/10.1016/j.neuropharm.2014.12.006 PMID: 25529272
2. Nys M, Kesters D, Ulens C. Structural insights into Cys-loop receptor function and ligand recognition. Biochem Pharmacol. 2013; 86(8):1042–53. https://doi.org/10.1016/j.bcp.2013.07.001 PMID: 23850718
3. Nemecz Á, Prevost Marie S, Menny A, Corringer P-J. Emerging molecular mechanisms of signal transduction in pentameric ligand-gated ion channels. Neuron. 2016; 90(3):452–70. https://doi.org/10.1016/j.neuron.2016.03.032 PMID: 27151638
4. Van Arnam EB, Dougherty DA. Functional probes of drug-receptor interactions implicated by structural studies: Cys-loop receptors provide a fertile testing ground. J Med Chem. 2014; 57:6289–300. https://doi.org/10.1021/jm500023m PMID: 24568098
5. Gotti C, Zoli M., Clementi F. Brain nicotinic acetylcholine receptors: native subtypes and their relevance. Trends Pharmacol Sci. 2006; 27:482–91. https://doi.org/10.1016/j.tips.2006.07.004 PMID: 16876883
6. Jensen AA, Frølund B, Liljefors T, Krogsgaard-Larsen P. Neuronal nicotinic acetylcholine receptors: Structural revelations, target identifications and therapeutic inspirations. J Med Chem. 2005; 48:4705–45. https://doi.org/10.1021/jm040219e PMID: 16033252
7. Dent JA. The evolution of pentameric ligand-gated ion channels. Adv Exp Med Biol. 2010; 683:11–23. https://doi.org/10.1007/978-1-4419-6445-8_2 PMID: 20737785
8. Barrantes FJ. Phylogenetic conservation of protein–lipid motifs in pentameric ligand-gated ion channels. Biochim Biophys Acta (BBA)—Biomembranes. 2015; 1848(9):1796–805. https://doi.org/10.1016/j.bbamem.2015.03.028 PMID: 25839355
9. Poveda JA, Marcela Giudici A, Lourdes Renart M, Morales A, González-Ros JM. Towards understanding the molecular basis of ion channel modulation by lipids: Mechanistic models and current paradigms. Biochim Biophys Acta (BBA)—Biomembranes. 2017; 1859:1507–16. https://doi.org/10.1016/j.bbamem.2017.04.003 PMID: 28408206
10. Duncan AL, Song W, Sansom MSP. Lipid-dependent regulation of ion channels and G protein-coupled receptors: Insights from structures and simulations. Annu Rev Pharmacol Toxicol. 2019; 60:31–50. https://doi.org/10.1146/annurev-pharmtox-010919-023411 PMID: 31506010
11. Baenziger JE, Miller KW, Rothschild KJ. Fourier transform infrared difference spectroscopy of the nicotinic acetylcholine receptor: Evidence for specific protein structural changes upon desensitisation. Biochem. 1993; 32:5448–54.
12. Criado M, Eibl H, Barrantes FJ. Effects of lipids on acetylcholine receptor. Essential need of cholesterol for maintenance of agonist-induced state transitions in lipid vesicles. Biochemistry. 1982; 21:3622–9. https://doi.org/10.1021/bi00258a015 PMID: 7115688
13. Fong TM, McNamee MG. Correlation between acetylcholine receptor function and structural properties of membranes. Biochemistry. 1986; 25:830–40. https://doi.org/10.1021/bi00352a015 PMID: 3008814
14. daCosta CJB, Ogrel AA, McCardy EA, Blanton MP, Baenziger JE. Lipid-protein interactions at the nicotinic acetylcholine receptor: A functional coupling between nicotinic receptors and phosphatidic acid-containing lipid bilayers. J Biol Chem. 2002; 277(1):201–8. https://doi.org/10.1074/jbc.M108341200 PMID: 11682482
15. Hamouda AK, Chiara DC, Sauls D, Cohen JB, Blanton MP. Cholesterol Interacts with transmembrane α-Helices M1, M3, and M4 of the torpedo nicotinic acetylcholine receptor: Photolabeling studies using [3H]azicholesterol. Biochemistry. 2006; 45(3):976–86. https://doi.org/10.1021/bi051978h PMID: 16411773
16. Hénault CM, Sun J, Therien JPD, daCosta CJB, Carswell CL, Labriola JM, et al. The role of the M4 lipid-sensor in the folding, trafficking, and allosteric modulation of nicotinic acetylcholine receptors. Neuropharmacol. 2015; 96:157–68.
17. Hénault CM, Govaerts C, Spurny R, Brams M, Estrada-Mondragon A, Lynch J, et al. A lipid site shapes the agonist response of a pentameric ligand-gated ion channel. Nat Chem Biol. 2019; 15:1156–64. https://doi.org/10.1038/s41589-019-0369-4 PMID: 31591563

18. Lee YH, Li L, Lasalde J, Rojas L, McNamee M, Ortiz-Miranda SI, et al. Mutations in the M4 domain of Torpedo californica acetylcholine receptor dramatically alter ion channel function. Biophys J. 1994; 66 (3, Part 1):646–53. https://doi.org/10.1016/s0006-3495(94)80838-0 PMID: 7516721

19. Lasalde JA, Tamamizu S, Butler DH, Vibat CRT, Hung B, McNamee MG. Tryptophan substitutions at the lipid-exposed transmembrane segment m4 of torpedo californica acetylcholine receptor govern channel gating. Biochemistry. 1996; 35(45):14139–48. https://doi.org/10.1021/bi961583l PMID: 8916899

20. Bouzat C, Roccamo AM, Garbus I, Barrantes FJ. Mutations at lipid-exposed residues of the acetylcholine receptor affect its gating kinetics. Mol Pharm. 1998; 54(1):146. https://doi.org/10.1124/mol.54.1.146 PMID: 9658200

21. Carswell CL, Sun J, Baenziger JE. Intramembrane aromatic interactions influence the lipid sensitivities of pentameric ligand-gated ion channels. J Biol Chem. 2015; 290:2496–507. https://doi.org/10.1074/jbc.M114.624395 PMID: 25519904

22. Haeger S, Kuzmin D, Detro-Dassen S, Lang N, Kilb M, Tsetlin V, et al. An intramembrane aromatic network determines pentameric assembly of Cys-loop receptors. Nat Struct Mol Biol. 2010; 17(1):90–8. https://doi.org/10.1038/nsmb.1721 PMID: 20023641

23. Laverty D, Desai R, Uchański T, Masiulis S, Stec WJ, Malinauskas T, et al. Cryo-EM structure of the human α1β3γ2 GABAA receptor in a lipid bilayer. Nature. 2019; 565(7740):516–20. https://doi.org/10.1038/s41586-018-0833-4 PMID: 30602789

24. Bocquet N, Nury H, Baaden M, Le Poupon C, Changeux J-P, Delarue M, et al. X-ray structure of a pentameric ligand-gated ion channel in an apparently open conformation. Nature. 2009; 457(7225):111–4. https://doi.org/10.1038/nature07462 PMID: 18987633

25. Hu H, Ataka K, Menny A, Fourati Z, Sauguet L, Corringer P-J, et al. Electrostatics, proton sensor, and networks governing the gating transition in GLIC, a proton-gated pentameric ion channel. Proc Natl Acad Sci. 2018; 115(52):E12172. https://doi.org/10.1073/pnas.1813378116 PMID: 30541892

26. Althoff T, Hibbs RE, Banerjee S, Gouaux E. X-ray structures of GluCl in apo states reveal a gating mechanism of Cys-loop receptors. Nature. 2014; 512(7514):333–7. https://doi.org/10.1038/nature13669 PMID: 25143115

27. Huang X, Chen H, Shaffer PL. Crystal structures of human GlyRα3 bound to ivermectin. Structure. 2017; 25(6):945–50.e2. https://doi.org/10.1016/j.str.2017.04.007 PMID: 28479061

28. Du J, Lu W, Wu S, Cheng Y, Gouaux E. Glycine receptor mechanism elucidated by electron cryomicroscopy. Nature. 2015; 526(7572):224–9. https://doi.org/10.1038/nature14853 PMID: 26344198

29. Hibbs R, Gouaux E. Principles of activation and permeation in an anion-selective Cys-loop receptor. Nature. 2011; 474:54–60. https://doi.org/10.1038/nature10139 PMID: 21572436

30. Laverty D, Thomas P, Field M, Andersen OJ, Gold MG, Biggin PC, et al. Crystal structures of a GABAA-receptor chimera reveal new endogenous neurosteroid-binding sites. Nat Struct Mol Biol. 2017; 24:977. https://doi.org/10.1038/nsmb.3477 PMID: 28967882

31. Walsh RM, Roh S-H, Gharpure A, Morales-Perez CL, Teng J, Hibbs RE. Structural principles of distinct assemblies of the human α4β2 nicotinic receptor. Nature. 2018; 557(7704):261–5. https://doi.org/10.1038/s41586-018-0081-7 PMID: 29720657

32. Corradi V, Sejdiu BI, Mesa-Galloso H, Abdizadeh H, Noskov SY, Marrink SJ, et al. Emerging diversity in lipid–protein interactions. Chem Rev. 2019; 119(9):5775–848. https://doi.org/10.1021/acs.chemrev.8b00451 PMID: 30758191

33. Hedger G, Sansom MSP. Lipid interaction sites on channels, transporters and receptors: Recent insights from molecular dynamics simulations. Biochim Biophys Acta. 2016; 1858:2390–400. https://doi.org/10.1016/j.bbamem.2016.02.037 PMID: 26946244

34. de Jong DH, Baoukina S, Ingólfsson HI, Marrink SJ. Martini straight: Boosting performance using a shorter cutoff and GPUs. Comp Phys Comms. 2016; 199:1–7.

35. Domicevica L, Koldsø H, Biggin PC. Multiscale molecular dynamics simulations of lipid interactions with P-glycoprotein in a complex membrane. J Mol Graph Mod. 2017; 77:250–8.

36. Duncan AL, Reddy T, Koldsø H, Hélie J, Fowler PW, Chavent M, et al. Protein crowding and lipid complexity influence the nanoscale dynamic organization of ion channels in cell membranes. Sci Reps. 2017; 7(1):16647. https://doi.org/10.1038/s41598-017-16865-6 PMID: 29192147

37. Song W, Yen H-Y, Robinson CV, Sansom MSP. State-dependent lipid interactions with the A2a receptor revealed by md simulations using in vivo-mimetic membranes. Structure. 2019; 27(2):392–403.e3. https://doi.org/10.1016/j.str.2018.10.024 PMID: 30581046

38. Basak S, Gicheru Y, Rao S, Sansom MSP, Chakrapani S. Cryo-EM reveals two distinct serotonin-bound conformations of full-length 5-HT3A receptor. Nature. 2018; 563(7730):270–4. https://doi.org/10.1038/s41586-018-0660-7 PMID: 30401837

39. Dämgen MA, Biggin PC. A refined open state of the glycine receptor obtained via molecular dynamics simulations. Structure. 2020; 28:1–10. https://doi.org/10.1016/j.str.2019.12.004 PMID: 31951536

40. Cheng MH, Xu Y, Tang P. Anionic lipid and cholesterol interactions with α4β2 nAChR: Insights from MD simulations. J Phys Chem B. 2009; 113(19):6964–70. https://doi.org/10.1021/jp900714b PMID: 19419220

41. Hénin J, Salari R, Murlidaran S, Brannigan G. A predicted binding site for cholesterol on the GABAA receptor. Biophys J. 2014; 106(9):1938–49. https://doi.org/10.1016/j.bpj.2014.03.024 PMID: 24806926

42. Sharp L, Salari R, Brannigan G. Boundary lipids of the nicotinic acetylcholine receptor: Spontaneous partitioning via coarse-grained molecular dynamics simulation. Biochimica et Biophysica Acta (BBA)—Biomembranes. 2019; 1861(4):887–96. https://doi.org/10.1016/j.bbamem.2019.01.005 PMID: 30664881

43. Ingólfsson HI, Carpenter TS, Bhatia H, Bremer P-T, Marrink SJ, Lightstone FC. Computational lipidomics of the neuronal plasma membrane. Biophys J. 2017; 113(10):2271–80. https://doi.org/10.1016/j.bpj.2017.10.017 PMID: 29113676

44. Huang X, Chen H, Michelsen K, Schneider S, Shaffer PL. Crystal structure of human glycine receptor alpha3 bound to antagonist strychnine. Nature. 2015; 526(7572):277–80. https://doi.org/10.1038/nature14972 PMID: 26416729

45. Burzomato V, Beato M, Groot-Kormelink PJ, Colquhoun D, Sivilotti LG. Single-channel behavior of heteromeric α1β glycine receptors: An attempt to detect a conformational change before the channel opens. J Neurosci. 2004; 24(48):10924–40. https://doi.org/10.1523/JNEUROSCI.3424-04.2004 PMID: 15574743

46. Sivilotti LG. What single-channel analysis tells us of the activation mechanism of ligand-gated channels: the case of the glycine receptor. J Physiol. 2010; 588(1):45–58. https://doi.org/10.1113/jphysiol.2009.178525 PMID: 19770192

47. Barrantes FJ. Structural basis for lipid modulation of nicotinic acetylcholine receptor function. Brain Research Reviews Chemical and Electrical Synapses. 2004; 47(1–3):71–95. https://doi.org/10.1016/j.brainresrev.2004.06.008 PMID: 15572164

48. Baenziger JE, Hénault CM, Therien JPD, Sun J. Nicotinic acetylcholine receptor–lipid interactions: Mechanistic insight and biological function. Biochim Biophys Acta Biomemb. 2015; 1848(9):1806–17. https://doi.org/10.1016/j.bbamem.2015.03.010 PMID: 25791350

49. Sooksawate T, Simmonds MA. Effects of membrane cholesterol on the sensitivity of the GABAA receptor to GABA in acutely dissociated rat hippocampal neurones. Neuropharmacology. 2001; 40(2):178–84. https://doi.org/10.1016/s0028-3908(00)00159-3 PMID: 11114396

50. daCosta CJB, Baenziger JE. A lipid-dependent uncoupled conformation of the acetylcholine receptor. J Biol Chem. 2009; 284:17819–25. https://doi.org/10.1074/jbc.M900030200 PMID: 19357079

51. Yu J, Zhu H, Lape R, Greiner T, Shahoei R, Wang Y, et al. Mechanism of gating and partial agonist action in the glycine receptor. bioRxiv. 2019:786632.

52. Morales-Perez CL, Noviello CM, Hibbs RE. X-ray structure of the human α4β2 nicotinic receptor. Nature. 2016; 538(7625):411–5. https://doi.org/10.1038/nature19785 PMID: 27698419

53. Hilf RJC, Dutzler R. X-ray structure of a prokaryotic pentameric ligand-gated ion channel. Nature. 2008; 452(7185):375–9. https://doi.org/10.1038/nature06717 PMID: 18322461

54. Safar F, Hurdiss E, Erotocritou M, Greiner T, Lape R, Irvine MW, et al. The startle disease mutation E103K impairs activation of human homomeric α1 glycine receptors by disrupting an intersubunit salt bridge across the agonist binding site. J Biol Chem. 2017; 292:5031–42. https://doi.org/10.1074/jbc.M116.767616 PMID: 28174298

55. Edgar RC. MUSCLE: Multiple sequence alignment with high accuracy and high throughput. Nucleic Acids Research. 2004; 32(5):1792–7. https://doi.org/10.1093/nar/gkh340 PMID: 15034147

56. Webb B, Sali A. Comparative protein structure modeling using modeller. Curr Prot Bioinf. 2014; 5:5.61–5.6.32.

57. Shen MY, Sali A. Statistical potential for assessment and prediction of protein structures. Protein Sci. 2006; 15(11):2507–24. https://doi.org/10.1110/ps.062416606 PMID: 17075131

58. Benkert P, Kunzli M, Schwede T. QMEAN server for protein model quality estimation. Nucleic Acids Res. 2009. https://doi.org/10.1093/nar/gkp322 PMID: 19429685

59. Abraham MJ, Murtola T, Schulz R, Páll S, Smith JC, Hess B, et al. GROMACS: High performance molecular simulations through multi-level parallelism from laptops to supercomputers. SoftwareX. 2015; 1–2:19–25.

60. Wassenaar TA, Ingólfsson HI, Böckmann RA, Tieleman DP, Marrink SJ. Computational lipidomics with insane: A versatile tool for generating custom membranes for molecular simulations. J Chem Theor Comput. 2015; 11:2144–55. https://doi.org/10.1021/acs.jctc.5b00209 PMID: 26574417

61. de Jong DH, Singh G, Bennett WFD, Arnarez C, Wassenaar TA, Schäfer LV, et al. Improved parameters for the martini coarse-grained protein force field. J Chem Theory Comput. 2013; 9(1):687–97. https://doi.org/10.1021/ct300646g PMID: 26589065

62. Periole X, Cavalli M, Marrink S-J, Ceruso MA. Combining an elastic network with a coarse-grained molecular force field: Structure, dynamics, and intermolecular recognition. J Chem Theory Comput. 2009; 5:2531–43. https://doi.org/10.1021/ct9002114 PMID: 26616630

63. Wassenaar TA, Pluhackova K, Böckmann RA, Marrink SJ, Tieleman DP. Going backward: A flexible geometric approach to reverse transformation from coarse grained to atomistic models. J Chem Theor Comput. 2014; 10(2):676–90. https://doi.org/10.1021/ct400617g PMID: 26580045

64. Lindorff-Larsen K, Piana S, Palmo K, Maragakis P, Klepeis J, Dror R, et al. Improved side-chain torsion potentials for the Amber ff99SB protein force field. Proteins: Struc Func Genet. 2010; 78:1950–8.

65. Jorgensen WL, Chandresekhar J, Madura JD, Impey RW, Klein ML. Comparison of simple potential functions for simulating liquid water. J Chem Phys 1983; 79:926–35.

66. Jämbeck JPM, Lyubartsev AP. Another piece of the membrane puzzle: Extending Slipids further. J ChemTheory Comp. 2013; 9(1):774–84.

67. Jämbeck JPM, Lyubartsev AP. An extension and further validation of an all-atomistic force field for biological membranes. J ChemTheory Comp. 2012; 8(8):2938–48.

68. Jämbeck JPM, Lyubartsev AP. Derivation and systematic validation of a refined all-atom force field for phosphatidylcholine lipids. J Phys Chem B. 2012; 116(10):3164–79. https://doi.org/10.1021/jp212503e PMID: 22352995

69. Horn AHC. A consistent force field parameter set for zwitterionic amino acid residues. J Mol Mod. 2014; 20(11):2478. https://doi.org/10.1007/s00894-014-2478-z PMID: 25338816

70. Bussi G, Donadio D, Parrinello M. Canonical sampling through velocity rescaling. J Chem Phys. 2007;126. https://doi.org/10.1063/1.2408420 PMID: 17212484

71. Parinello M, Rahman A. Polymorphic transitions in single crystals—a new molecular dynamics method. J Appl Phys. 1981; 52:7182–90.

72. Essman U, Perera L, Berkowitz ML, Darden T, Lee H, Pedersen LG. A smooth particle mesh Ewald method. J Chem Phys. 1995; 103:8577–93.

73. Darden T, York D, Pedersen L. Particle mesh Ewald—an N.log(N) method for Ewald sums in large systems. J Chem Phys. 1993; 98:10089–92.

74. Hess B, Bekker J, Berendsen HJC, Fraaije JGEM. LINCS: A linear constraint solver for molecular simulations. J Comp Chem. 1997; 18:1463–72.

75. Michaud-Agrawal N, Denning EJ, Woolf T, Beckstein O. MDAnalysis: A toolkit for the analysis of molecular dynamics simulations. J Comput Chem. 2011; 32:2319–27. https://doi.org/10.1002/jcc.21787 PMID: 21500218

76. McGibbon RT, Beauchamp KA, Harrigan MP, Klein C, Swails JM, Hernandez CX, et al. MDTraj: A modern open library for the analysis of molecular dynamics trajectories. Biophys J. 2015; 109:1528–32. https://doi.org/10.1016/j.bpj.2015.08.015 PMID: 26488642

77. Humphrey W, Dalke A, Schulten K. VMD—Visual molecular dynamics. J Mol Graph. 1996; 14:33–8. https://doi.org/10.1016/0263-7855(96)00018-5 PMID: 8744570